General Synergic and Distributed Planning Models of Natural Gas and Electricity Systems and Integrated Energy Systems

Ang Xuan, Jing Xiao and Puming Xu

June 7, 2021

General Synergic and Distributed Planning Models of Natural Gas and Electricity Systems and Integrated Energy Systems

1st Ang Xuan
Tsinghua-Berkeley Shenzhen Institute, Tsinghua University
Shenzhen, China
xa19@mails.tsinghua.edu.cn

2nd Jing Xiao*
Hunan Electric Power Research Institute
State Grid Hunan Electric Power Company
Changsha, China
xiaoj72@hn.sgcc.com.cn

3rd Puming Xu
Hunan Electric Power Research Institute
State Grid Hunan Electric Power Company
Changsha, China
xupm@hn.sgcc.com.cn

***Abstract*—Integrated energy system coupling with multi-energy devices, energy storage systems, and renewable energy systems is regarded as one of the most promising solutions for future energy systems. A general synergic planning model considering expansion of electricity system, natural gas system, and interior structure and site selection of integrated energy systems is proposed in this paper. Moreover, the joint planning model is decomposed into three planning sub-problems to represent different ownerships of the three agents, and the alternating direction method of multipliers (ADMM) is adopted to solve the tripartite distributed planning problem. Finally, the effectiveness of the planning method is verified on the updated version of IEEE RTS 24-bus electric system, Belgian 20-node natural gas system, and two assumed integrated energy systems.**

Keywords—synergic planning, distributed planning, expansion planning, integrated energy system, alternating direction method of multipliers

I. Introduction

As the world moves away from its total reliance on fossil energy, integrated energy systems (IESs), in which electricity, gas, heating, and cooling interact with one another, have come to be regarded as one of the most promising solutions for future energy systems [1]. The penetration of intermittent renewable energy systems (RESs) such as photovoltaics and wind power has been receiving more and more attention in recent years [2]. At the same time, energy storage systems (ESSs) [3] are vital in alleviating fluctuation of renewable energy and load, and can provide peak shaving, uninterruptible power supply, energy arbitrage, etc. Moreover, the energy hub (EH) concept has been introduced as a tool to model IES in the project "Vision of Future Energy Systems" [4]. An EH takes in energy at input ports connected to electricity and gas systems and provides output energy such as electricity, gas, heating, and cooling, so that the EH is a considered an option for IES planning.

IES planning requires comprehensive consideration of all involved energy systems at once. There have been several reports in recent years of work focusing on IES planning with multiple energy systems. In configuring district EHs, one paper [5] proposed a planning model for a district energy sector, and another paper [6] presented a two-stage mixed-integer linear programming (MILP) approach for district-level IES planning, considering component and capacity selections. These reports all focused on the interior structure of a single EH and ignored siting problems. There have also been various reports on synergic planning of energy systems such as electricity and natural gas systems. Expansion planning of integrated electricity and natural gas systems was presented in papers [7] and [8]. Also, various synergic operation models have been applied to IES planning, such as a bi-level synergic planning framework [9], a two-stage stochastic planning framework [10], and a robust synergic planning framework [11].

However, the above research projects have addressed only one, or perhaps a few, of the problems associated with expanding IES, such as siting and selecting IES equipment capacity. Little work has been reported on formulating a general synergic planning strategy taking account of all the sub-problems.

Past synergic planning has assumed that electricity systems (ESs), natural gas systems (GSs), and IESs are owned and operated by a single stakeholder, which does not reflect the actual situation. It is more practicable to divide the problem into three independent parts in light of the actual circumstances encountered in a distributed optimization framework. To address the ES-GS-IES tripartite model, a distributed algorithm, the Alternating Direction Method of Multipliers (ADMM) [12], is employed in this paper. ADMM brings in dual multipliers to relax equality constraints and to decompose the overall problem into multiple independent sub-problems—or blocks—such that the variables and constraints of one sub-problem will be distinct from those in others. Published reports [13] show that the three-block ADMM still globally converges with any penalty parameter larger than zero if the third objective function is smooth and strongly convex.

The main contributions of this paper are summarized as follows:

1) A synergic planning model is proposed considering GS/ES expansion, IES siting, and IES interior equipment type and capacity selection.
2) A 3-agent (GS+ES+IES) distributed planning model is proposed, in which the GS, ES, and IES are owned and operated by different stakeholders and ADMM is employed to solve the three-agent distributed optimization problem.

II. Model Formulation

A. GS model

A typical natural gas system consists of natural gas sources, compressors, natural gas transmission pipelines, and gas loads.

1) Natural gas sources:

$$\underline{P_s} \le p_{s,t} \le \overline{P_s}, \quad \forall s \in \Omega_{GS} \tag{1}$$

$$-RD_s \le p_{s,t} - p_{s,t\text{-}1} \le RU_s, \quad \forall s \in \Omega_{GS}, \forall t \in [2,T] \tag{2}$$

The production of natural gas sources is limited by output constraints (1) and ramp constraints (2).

2) Natural gas transmission pipeline:

The Weymouth equation (3) is adopted to express the natural gas transmission pipeline flow in this model, in which the gas flow is relatively nonconvex and proportional to the square of the nodal gas pressure. The piecewise linearization method that we adopt can be found in reference [14], and corresponding formulas are listed as (4)-(8).

$$F_{p,t}\left|F_{p,t}\right| = W_p^2\left(I_{from,t}{}^2 - I_{to,t}{}^2\right), \forall p \in \Omega_{EP} \tag{3}$$

$$I_{m,t} = \pi^2_{m,t}, \forall m \in \Omega_{GN} \tag{4}$$

$$\underline{\pi_m} \le \pi_{m,t} \le \overline{\pi_m}, \forall m \in \Omega_{GN} \tag{5}$$

$$F_{p,t} = F_{p,t,1} + \sum_{k=1}^{segment} \delta_{p,t,k}\left(F_{p,t,k+1} - F_{p,t,k}\right), \forall p \in \Omega_{EP} \tag{6}$$

$$F_{p,t}\left|F_{p,t}\right| = F_{p,t,1}\left|F_{p,t,1}\right| + \sum_{k=1}^{segment} \delta_{p,t,k}\left(F_{p,t,k+1}\left|F_{p,t,k+1}\right| - F_{p,t,k}\left|F_{p,t,k}\right|\right), \forall p \in \Omega_{EP} \tag{7}$$

$$0 \le \delta_{p,t,k} \le 1, \forall k = [1, segment] \tag{8}$$

$$\phi_{p,t,k} \le \delta_{p,t,k}, \forall k = [1, segment] \tag{9}$$

$$\delta_{p,t,k+1} \le \phi_{p,t,k}, \forall k = [1, segment-1] \tag{10}$$

Expressions (9)-(10) are gas-flow constraints for existing gas pipelines. (9) implies that the gas flow will not satisfy the Weymouth equation if the compressor is chosen to invest. M is a large positive integer in the large-M method to ensure that the gas flow will be zero when a candidate pipeline is not built (11). y is a binary variable to indicate the state of the candidate pipeline in (12). (13) introduces the variable I to replace nodal pressure π to in order to avoid a quadratic equation.

$$-y_p^{com}M \le F_{p,t}\left|F_{p,t}\right| - W_p^2\left(I_{from,t}{}^2 - I_{to,t}{}^2\right) \le y_p^{com}M, \forall p \in \Omega_{EP} \tag{11}$$

$$-\overline{F_p} \le F_{p,t} \le \overline{F_p}, \forall p \in \Omega_{EP} \tag{12}$$

$$\begin{aligned}&-(1+y_p^{com}-y_p)M_g \le F_{p,t}\left|F_{p,t}\right| - W_p^2\left(\pi_{from,t}{}^2 - \pi_{to,t}{}^2\right)\\ &\le (1+y_p^{com}-y_p)M_g, \forall p \in \Omega_{CP}\end{aligned} \tag{13}$$

$$-y_p\overline{F_p} \le F_{p,t} \le y_p\overline{F_p}, \forall p \in \Omega_{CP} \tag{14}$$

B. ES model

A typical electricity system composes generators, electricity transmission lines, and electricity loads.

1) Generators:

$$u_{j,t}\underline{P_{j,t}} \le P_{j,t} \le u_{j,t}\overline{P_{j,t}}, \forall j \in \Omega_{GEN} \tag{15}$$

$$-RD_j \le P_{j,t} - P_{j,t-1} \le RU_j, \forall j \in \Omega_{GEN}, \forall t \in [2,T] \tag{16}$$

$$\sum_{tt=t-T_n^{on}+1}^{t} v_{j,tt} \le u_{j,t}, \forall j \in \Omega_{GEN}, \forall t \in \left[T_j^{on}, T\right] \tag{17}$$

$$\sum_{tt=t-T_n^{off}+1}^{t} w_{j,tt} \le 1 - u_{j,t}, \forall j \in \Omega_{GEN}, \forall t \in \left[T_j^{off}, T\right] \tag{18}$$

$$u_{j,t} - u_{j,t-1} = v_{j,t} - w_{j,t}, \forall j \in \Omega_{GEN}, \quad \forall t \in [2,T] \tag{19}$$

$$v_{j,t} + w_{j,t} \le 1, \forall j \in \Omega_{GEN}, \quad \forall t \in [2,T] \tag{20}$$

The unit commitment constraints (15)-(20) are employed to accurately describe generators' output characteristics. u is a binary variable to indicate the operational state of the generator in (15). (16) gives ramp-up power and ramp-down power constraints for generators. (17)-(20) are minimum uptime and downtime constraints, where v and w are binary variables to reflect startup and shutdown actions. The value of v turns out to be 1 if the generator started up at the last moment; the value of w turns out to be 1 if the generator shut down at the last moment. Otherwise these quantities are zero.

2) Electricity transmission lines:

$$F_{l,t} = \frac{\theta_{from,t} - \theta_{to,t}}{x_l}, \forall l \in \Omega_{EL} \tag{21}$$

$$-(1-y_l)M_E \le F_{l,t} - \frac{\theta_{from,t} - \theta_{to,t}}{x_l} \le (1-y_l)M_E, \forall l \in \Omega_{CL} \tag{22}$$

$$-\overline{F_l} \le F_{l,t} \le \overline{F_l}, \forall l \in \Omega_{EL} \tag{23}$$

$$-y_l\overline{F_l} \le F_{l,t} \le y_l\overline{F_l}, \forall l \in \Omega_{CL} \tag{24}$$

$$-\pi \le \theta_{n,t} \le \pi, \forall n \in \Omega_{EB} \tag{25}$$

It is acceptable for the DC power flow model to be adopted to estimate a steady state for the distribution system. M_E in (22) is set to be $2\pi / x_l$ to ensure that power flow is zero if the transmission line l is not built. (23)-(25) are constraints for power flow on an existing transmission line, power flow on a candidate transmission line, and nodal phase, respectively.

C. IES model

The equipment to be planned in an IES can be divided into three types: multi-energy coupling device (combined cooling, heating and power, gas boiler, air conditioner, electric boiler, etc.); RES (photovoltaics, wind power); and ESS (battery energy storage system, thermal energy storage system, cold energy storage system).

1) Multi-energy coupling device component:

$$\begin{aligned}&L_{h,k,t} = C_{k,can}P_{h,Can,t}\\ &k \in \{e,h,c,g\}\end{aligned} \tag{26}$$

$$\begin{aligned}&0 \le P_{h,can,t} \le y_{h,can}\overline{P_{h,can,t}}\\ &\forall can \in \{TL, TP, CCHP, GB, AC\}, \forall h \in \Omega_{EH}\end{aligned} \tag{27}$$

The relationship between input and output power of one multi-energy coupling device is linearized in matrix form based on EH theory [4] in (26). Energy forms include electricity, heating, cooling, and gas in one IES. Input power is constrained in (27), where a candidate can be chosen from electricity transmission line (TL), gas transmission pipeline (TP), combined cooling, heating and power (CCHP), gas boiler (GB), air conditioner (AC), electric boiler (EB), etc.

2) RES component:

$$0 \le P_{RES,t} \le y_{RES} \overline{P_{RES,t}^{e,out}} \quad RES \in \{WT, PV\} \tag{28}$$

The actual operational power of renewables is ruled by maximum output power in (28), where the integer decision variable y_{RC} indicates the number of RES component modules to be planned.

3) ESS component:

$$0 \le P_{ESS,t}^{ch} \le y_{ESS} \overline{P_{ESS}^{ch}} \tag{29}$$

$$0 \le P_{ESS,t}^{dis} \le y_{ESS} \overline{P_{ESS}^{dis}} \tag{30}$$

$$0 \le P_{ESS,t}^{ch} \le \upsilon_{ESS,t}^{ch} M \tag{31}$$

$$0 \le P_{ESS,t}^{dis} \le \upsilon_{ESS,t}^{dis} M \tag{32}$$

$$\upsilon_{ESS,t}^{ch} + \upsilon_{ESS,t}^{dis} \le 1 \tag{33}$$

$$y_{ESS} \underline{SOC_{ESS}} \le SOC_{ESS,t} \le y_{ESS} \overline{SOC_{ESS}} \tag{34}$$

$$SOC_{ESS,t} = SOC_{ESS,t-1} + \eta_{ESS}^{ch} P_{ESS,t}^{in} - P_{ESS,t}^{dis} / \eta_{ESS}^{dis} \tag{35}$$

$$SOC_{ESS,1} = SOC_{ESS,T} \quad ESS \in \{BESS, TESS, CESS\} \tag{36}$$

Charging/discharging powers of ESSs are limited by the power of investment option in (29)-(32), in which the upper bound is denoted by the integer variable y_{ESS}, the number of ESSs module and binary variable $v_{s,t}^{ch,n} / v_{s,t}^{dis,n}$ denoting the charge/discharge states, while M is a large number used in the "Big-M" method. Constraint (33) ensures that the ESSs cannot be charged and discharged at the same time. Constraint (34), representing the state of charge (SOC), is limited by the number of ESS modules and the energy capacity of one module. Constraint (35) denotes the relationship between charge/discharge power and SOC. Constraint (36) ensures that the initial and final states of SOC are the same.

4) Load power balance:

$$L_{e,t} - P_{BESS,t}^{ch} + P_{BESS,t}^{dis} + P_{WT,t} + P_{PV,t} = L_{e,t}^{load} \tag{37}$$

$$L_{h,t} - P_{TESS,t}^{ch} + P_{TESS,t}^{dis} = L_{h,t}^{load} \tag{38}$$

$$L_{c,t} - P_{CESS,t}^{ch} + P_{CESS,t}^{dis} = L_{c,t}^{load} \tag{39}$$

$$L_{g,t} = L_{g,t}^{load} \tag{40}$$

(37)-(40) are the power balance constraints on the supply side.

5) IES siting:

$$\sum_m s_{m,h} \ge 1, \forall m \in \Omega_{GN}, \forall h \in \Omega_{EH} \tag{41}$$

$$0 \le T_{m,h,t}^{g} \le s_{m,h} M, \forall m \in \Omega_{GN}, \forall h \in \Omega_{EH} \tag{42}$$

$$\sum_n s_{n,h} \ge 1, \forall n \in \Omega_{EN}, \forall h \in \Omega_{EH} \tag{43}$$

$$0 \le T_{n,h,t}^{e} \le s_{n,h} M, \forall n \in \Omega_{EN}, \forall h \in \Omega_{EH} \tag{44}$$

III. Methodology

The constraints presented above include natural gas source constraints, Weymouth linearized gas transmission constraints, generator unit commitment constraints, electricity transmission constraints, energy hub component constraints, and energy hub load balance constraints. We bring in continuous variables P and P' to represent the transmission power outputted from GS/ES and inputted to IES.

$$A_{m,s} P_{s,t} + \sum_{p \in \Omega_{EP}} B_{m,p} F_{p,t} + \sum_{p \in \Omega_{CP}} B_{m,p} F_{p,t} = \sum_h T_{m,h,t}^{g} + L_{m,t}, \forall m \in \Omega_{GN}, \forall s \in \Omega_{GS}, \forall h \in \Omega_{EH} \tag{45}$$

$$C_{n,j} P_{j,t} + \sum_{l \in \Omega_{EL}} D_{n,l} F_{l,t} + \sum_{l \in \Omega_{CL}} D_{n,l} F_{l,t} = \sum_h T_{n,h,t}^{e} + L_{n,t}, \forall n \in \Omega_{EN}, \forall j \in \Omega_{GEN}, \forall h \in \Omega_{EH} \tag{46}$$

$$\sum_m T'^{g}_{m,h,t} = P_{h,CCHP,t} + P_{h,GB,t} + P_{h,TP,t}, \forall m \in \Omega_{GN}, \forall h \in \Omega_{EH} \tag{47}$$

$$\sum_n T'^{e}_{n,h,t} = P_{h,TL,t} + P_{h,AC,t}, \forall n \in \Omega_{EN}, \forall h \in \Omega_{EH} \tag{48}$$

The power balance at the GS-ES-IES tripartite interfaces can be modeled as (45)-(48). (45) and (46) are gas and electricity nodal power balance functions; (47) and (48) are power balance constraints on the input side for a single IES.

A. General Synergic Planning

The centralized planning model can be formulated as follows.

$$\min \left\{ \begin{aligned} & \sum_{p \in \Omega_{CP}} c_p y_p + \sum_{com \in \Omega_{COM}} c_{com} y_{com} + \sum_{l \in \Omega_{CL}} c_l y_l \\ & + \sum_t \left(\sum_{m \in \Omega_{GN}} c_m P_{m,t} + \sum_{n \in \Omega_{EN}} c_n P_{n,t} \right) \\ & + \sum_{h \in \Omega_{EH}} \left(\sum_{can} c_{can} y_{h,can} + \sum_{RES} c_{RES} y_{h,RES} + \sum_{ESS} c_{ESS} y_{h,ESS} \right) \\ & + \sum_{h \in \Omega_{EH}} \left(\sum_{m \in \Omega_{GN}} c_m s_{m,h} + \sum_{n \in \Omega_{EN}} c_n s_{n,h} \right) \\ & + \sum_t \sum_{h \in \Omega_{EH}} \left(c_{TP} P_{h,TP,t} + c_{TL} P_{h,TL,t} \right) \end{aligned} \right\} \tag{49}$$

$$T_{m,h,t}^{g} = T'^{g}_{m,h,t}, \forall m \in \Omega_{GN} \quad T_{n,h,t}^{e} = T'^{e}_{n,h,t}, \forall n \in \Omega_{EN} \tag{50}$$

s.t. (1)-(48)

The objective function (49) is intended to minimize the total investment cost and operation cost for GS, ES, and IES. The first three terms represent the investment cost of candidate transmission lines, pipelines, and compressors. The second term represents the operation cost of gas sources and generators. The last two terms represent the investment costs of IES components and siting. (50) ensures equal output and input power in the same channel; the formula connects three separate planning objectives directly.

B. General Distributed Planning: 3-block optimization

To some extent, synergic planning ignores the different ownership of tripartite systems, while distributed planning considers a more practical model. Three agents can be optimized separately to achieve optimal transmission power T/T'. Different from synergic planning in (50), ADMM-based distributed planning brings in auxiliary continuous variables $\tilde{T}^{g}_{m,h,t}$ between output power $T^{g}_{m,h,t}$ from GS and input power $T'^{g}_{m,h,t}$ to IES in GS-IES coupling system and $\tilde{T}^{e}_{n,h,t}$ between output power $T^{e}_{n,h,t}$ from ES and input power $T'^{e}_{n,h,t}$ to IES in ES-IES coupling system. Original objective functions are expanded to augmented Lagrange functions (ALF) with secondary penalty terms in (51) to (53).

$$\min L_{GN} = \min \left\{ \begin{array}{l} \sum_{p\in\Omega_{CP}} c_p y_p + \sum_{com\in\Omega_{COM}} c_{com} y_{com} + \sum_t \sum_{m\in\Omega_{GN}} c_m P_{m,t} \\ + \sum_t \sum_{h\in\Omega_{EH}} \sum_{m\in\Omega_{GN}} \lambda^{gn,k}_{m,h,t} \left(T^{g}_{m,h,t} - \tilde{T}^{g,k}_{m,h,t} \right) \\ + \rho^{gn}/2 \sum_t \sum_{h\in\Omega_{EH}} \sum_{m\in\Omega_{GN}} \left(T^{g}_{m,h,t} - \tilde{T}^{g,k}_{m,h,t} \right)^2 \end{array} \right\} \quad (51)$$

$$\min L_{EN} = \min \left\{ \begin{array}{l} \sum_{l\in\Omega_{CL}} c_l y_l + \sum_t \sum_{n\in\Omega_{EN}} c_n P_{n,t} \\ + \sum_t \sum_{h\in\Omega_{EH}} \sum_{n\in\Omega_{EN}} \lambda^{en,k}_{n,h,t} \left(T^{e}_{n,h,t} - \tilde{T}^{e}_{n,h,t} \right) \\ + \rho^{en}/2 \sum_t \sum_{h\in\Omega_{EH}} \sum_{n\in\Omega_{EN}} \left(T^{e}_{n,h,t} - \tilde{T}^{e}_{n,h,t} \right)^2 \end{array} \right\} \quad (52)$$

$$\min L_{EH} = \min \left\{ \begin{array}{l} \sum_{h\in\Omega_{EH}} \left(\sum_{can} c_{can} y_{h,can} + \sum_{RES} c_{RES} y_{h,RES} + \sum_{ESS} c_{ESS} y_{h,ESS} \right) \\ + \sum_{h\in\Omega_{EH}} \left(\sum_{m\in\Omega_{GN}} c_m s_{m,h} + \sum_{n\in\Omega_{EN}} c_n s_{n,h} \right) \\ + \sum_t \sum_{h\in\Omega_{EH}} \left(c_{TP} P_{h,TP,t} + c_{TL} P_{h,TL,t} \right) \\ + \sum_t \sum_{h\in\Omega_{EH}} \sum_{m\in\Omega_{GN}} \lambda^{ehg,k}_{m,h,t} \left(T'^{g}_{m,h,t} - \tilde{T}^{g}_{m,h,t} \right) \\ + \rho^{ehg}/2 \sum_t \sum_{h\in\Omega_{EH}} \sum_{m\in\Omega_{GN}} \left(T'^{g}_{m,h,t} - \tilde{T}^{g}_{m,h,t} \right)^2 \\ + \sum_t \sum_{h\in\Omega_{EH}} \sum_{n\in\Omega_{EN}} \lambda^{ehe,k}_{n,h,t} \left(T'^{e}_{n,h,t} - \tilde{T}^{e}_{n,h,t} \right) \\ + \rho^{ehe}/2 \sum_t \sum_{h\in\Omega_{EH}} \sum_{n\in\Omega_{EN}} \left(T'^{e}_{n,h,t} - \tilde{T}^{e}_{n,h,t} \right)^2 \end{array} \right\} \quad (53)$$

The distributed planning model framework is listed in TABLE I.

TABLE I. ADMM-BASED DISTRIBUTED PLANNING MODEL FRAMEWORK

Agent	GS	ES	IES
Objective Function	(51)	(52)	(53)
Power Balance Constraints	(45)	(46)	(47)-(48)
Other Constraints	s.t. (1)-(14)	s.t. (15)-(25)	s.t. (26)-(44)

The detailed process of the proposed ADMM-based ES-GS-IES 3-block distributed optimization algorithm is shown in TABLE II. The variables T/T', auxiliary variables $\tilde{T}$, and multipliers λ are updated alternatively.

TABLE II. ADMM-BASED DISTRIBUTED ALGORITHM

Algorithm: ADMM-Based ES-GS-IES 3-block distributed optimization

Stage 1: Initialization

Initialize multipliers $\lambda^{gn,k}_{m,h,t}, \lambda^{en,k}_{n,h,t}, \lambda^{ehg,k}_{m,h,t}, \lambda^{ehg,k}_{m,h,t}$ and auxiliary variables $\tilde{T}^{g}_{m,h,t}, \tilde{T}^{e}_{n,h,t}$, define epsilon convergence $\varepsilon^{g}, \varepsilon^{e}$.

Stage 2: Optimization

1 Optimize GS model.

$$T^{g,k+1}_{m,h,t} = \arg\min L_{GN}(T^{g,k}_{m,h,t}, \tilde{T}^{g,k}_{m,h,t}, \lambda^{gn,k}_{m,h,t})$$

2 Optimize ES model

$$T^{e,k+1}_{n,h,t} = \arg\min L_{EN}(T^{e,k}_{n,h,t}, \tilde{T}^{e,k}_{n,h,t}, \lambda^{en,k}_{n,h,t})$$

3 Optimize IES model.

$$\left\{ T'^{g,k+1}_{m,h,t}, T'^{e,k+1}_{n,h,t} \right\} = \arg\min$$
$$L_{EH}(T'^{g,k}_{m,h,t}, T'^{e,k}_{n,h,t}, \tilde{T}^{g,k}_{m,h,t}, \tilde{T}^{e,k}_{n,h,t}, \lambda^{ehg,k}_{m,h,t}, \lambda^{ehe,k}_{n,h,t})$$

Stage 3: Judgment

If $\max(\rho^{gn} \left| T^{g,k+1}_{m,h,t} - \tilde{T}^{g,k}_{m,h,t} \right|, \rho^{ehg} \left| T'^{g,k+1}_{m,h,t} - \tilde{T}^{g,k}_{m,h,t} \right|) \le \varepsilon^{g}$ &

$\max(\rho^{en} \left| T^{e,k+1}_{n,h,t} - \tilde{T}^{e,k}_{n,h,t} \right|, \rho^{ehe} \left| T'^{e,k+1}_{n,h,t} - \tilde{T}^{e,k}_{n,h,t} \right|) \le \varepsilon^{e}$,

Export the optimal solution. Finished.

Else update

$$\lambda^{gn,k+1}_{m,h,t} = \lambda^{gn,k}_{m,h,t} + \rho^{gn} \left(T^{g,k+1}_{m,h,t} - \tilde{T}^{g,k}_{m,h,t} \right)$$

$$\lambda^{en,k+1}_{n,h,t} = \lambda^{en,k}_{n,h,t} + \rho^{en} \left(T^{e,k+1}_{n,h,t} - \tilde{T}^{e,k}_{n,h,t} \right)$$

$$\lambda^{eng,k+1}_{m,h,t} = \lambda^{ehg,k}_{m,h,t} + \rho^{ehg} \left(T'^{g,k+1}_{m,h,t} - \tilde{T}^{g,k}_{m,h,t} \right)$$

$$\lambda^{ehe,k+1}_{n,h,t} = \lambda^{ehe,k}_{n,h,t} + \rho^{ehe} \left(T'^{e,k+1}_{n,h,t} - \tilde{T}^{e,k}_{n,h,t} \right)$$

$$\tilde{T}^{g,k+1}_{m,h,t} = \left(\rho^{gn} T^{g,k+1}_{m,h,t} + \rho^{ehg} T'^{g,k+1}_{m,h,t} \right) / \left(\rho^{gn} + \rho^{ehg} \right)$$

$$\tilde{T}^{e,k+1}_{n,h,t} = \left(\rho^{en} T^{e,k+1}_{n,h,t} + \rho^{ehe} T'^{e,k+1}_{n,h,t} \right) / \left(\rho^{en} + \rho^{ehe} \right)$$

Return to **Stage 2**

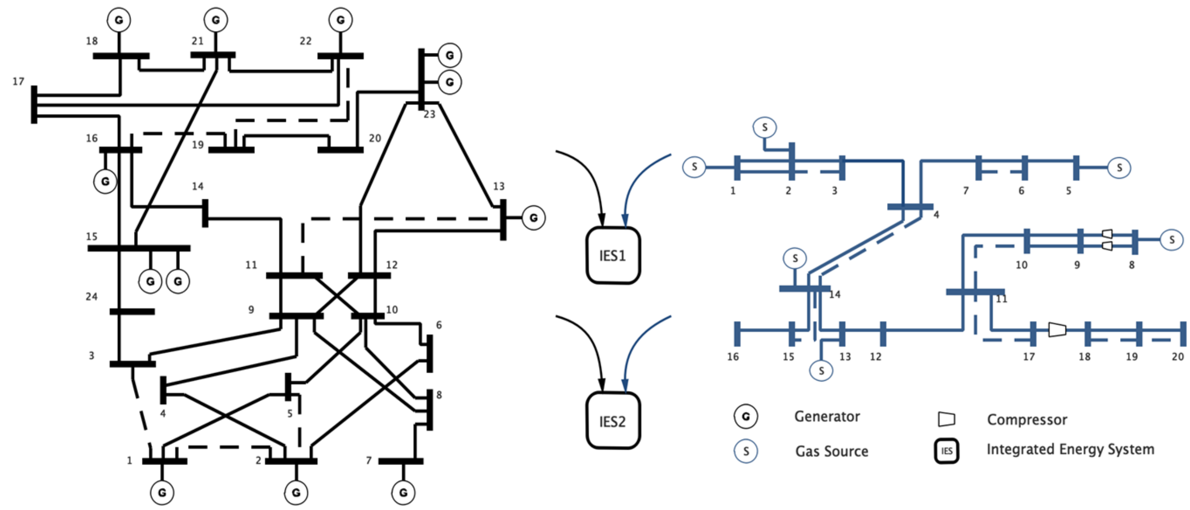

Figure 1. Planned model composed of updated IEEE RTS 24-bus electric system, Belgium 20-node natural gas system, and two assumed district IESs

IV. Case Study

An updated IEEE RTS 24-bus electric system, Belgium 20-node natural gas system, and two assumed integrated energy systems are employed to verify the effectiveness of the proposed synergic and distributed models, and datasets are available in [15]. The large mixed integer programming is modelled on Matlab 2020 with Yalmip and solved by Gurobi 9.1. $\rho^{gn}, \rho^{en}, \rho^{ehg}, \rho^{ehe}$ are set to 200, 200, 100, 100, respectively, and $\varepsilon^{g}, \varepsilon^{e}$ are set to 0.001.

The sketch map of expansion planning of GS/ES and siting planning of IESs is shown in Figure 1, while the design of IES internal components structure is shown in Figure 2. To verify the effectiveness and increase diversity, two IESs are assumed to have different load types, in which one is designed without cold load, another without heat load.

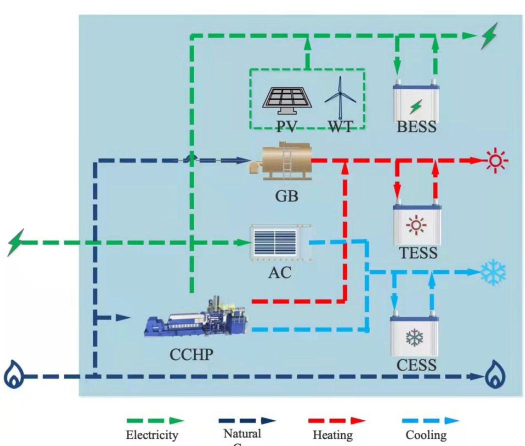

Figure 2. Designed IES intern components diagram

A. Expansion results and site selection

The detailed planning results obtained by two models are displayed in Table III. The two models adopted the same expansion decisions on pipelines, transmission lines, and compressors. This indicates that compared with the large system loads, several IES loads have limited influence on the expansion planning of GS and ES. As for the siting problems for IESs, big differences occurs at both IESs: IES1 is sited to bus 15 in ES and node 8 in GS; IES2 is sited to bus 23 in ES and node 2 in GS. The reason for this difference in site selections is the priority of planning by different stakeholders. For synergic planning, global economic optimality is achieved by the IES being sited on the load side due to the tradeoff between site selection costs and operation costs of generators and gas sources. IES's priority is to ensure the supply of multi-energy load; thus the site selections are at the source end of GN and EN.

Table III. Planning results obtained by two models

		Synergic planning	Distributed planning
Expansion	GS	Pipelines: All candidate pipelines Compressors: All candidate compressors	Pipelines: All candidate pipelines Compressors: All candidate compressors
	ES	19-22	19-22
Siting	IES1	GS:17 ES:3	GS:8 ES:15
	IES2	GS:17 ES:3	GS:2 ES:23
Investment Cost (M$)	GS	1.183	1.183
	ES	0.057	0.048
	IES	4.44	4.52
Operation Cost (M$)	GS	12.85	12.85
	ES	0.44	0.42
	IES	0.0016	0.0012
Total Cost (M$)		18.97	19.02 (+0.26%)

In terms of planning costs of the two approaches, a single stakeholder is assumed to own the whole GN-EN-IES in the synergic planning model, while GN-EN-IES possesses three separate ownerships in the distributed model. Moreover, in the iteration process, convergence means each stakeholder achieves a consensus in transmission power with acceptable accuracy ($\varepsilon^{g}, \varepsilon^{e}$). In contrast, total cost of distributed planning is 0.26% larger than the global economic optimal solution.

B. IES components planning results

IES components planning results are further analyzed in TABLE IV. The ESS and RES are not chosen by global economic optimality. Generators and gas sources tend to output more to reduce the extra investment cost of IES equipment. In the distributed model, the power supply of multi-energy load is prioritized, so that the stakeholder of IESs adopted more ESSs and RESs to increase the power supply flexibility.

TABLE IV. IES COMPONENTS OBTAINED BY TWO MODELS

		Synergic planning	Distributed planning
IES1	CCHP (MW)	1	1
	GB (MW)	4	4
	AC (MW)	0	0
	BESS (MWh)	0	0.5
	TESS (MWh)	0	0.3
	CESS (MWh)	0	0
	WT (MW)	0.2	0.6
	PV (MW)	0.1	0.2
IES2	CCHP (MW)	1	1
	GB (MW)	0	0
	AC (MW)	3	3
	BESS (MWh)	0	0.5
	TESS (MWh)	0	0
	CESS (MWh)	0	0.4
	WT (MW)	0.2	0.6
	PV (MW)	0.1	0.2

V. CONCLUSION

This paper proposes a synergic planning model and an ADMM-based distributed planning model considering GS and ES expansion, IESs siting and components. To sum up, the proposed synergic planning and ADMM-based distributed planning models ensure the power supply of electricity, gas, heat and cold load. The case study verified the effectiveness of the proposed model by carefully noting the differences between them. The planning results illustrate that whether the tripartite blocks are regarded as being owned by one stakeholder to achieve global economic optimality or owned by three stakeholders separately to achieve decision independence through transmission power convergence, both models have rationality and novelty. At the same time, case results proved the feasibility of the ADMM algorithm for 3-block distributed optimization. Our future work will focus on studying the influence of planning results of penalty term coefficients and improving the convergence speed and computational efficiency of the ADMM algorithm.

REFERENCES

[1] Mancarella, Pierluigi. "MES (multi-energy systems): An overview of concepts and evaluation models". Energy, vol.65, 2014, pp. 1-17. doi:10.1016/j.energy.2013.10.041

[2] Jurasz J, Canales F A, Kies A, et al. A review on the complementarity of renewable energy sources: Concept, metrics, application and future research directions[J]. Solar Energy, 2020, 195: 703-724.

[3] Zhang C, Wei Y L, Cao P F, et al. Energy storage system: Current studies on batteries and power condition system[J]. Renewable and Sustainable Energy Reviews, 2018, 82: 3091-3106.

[4] Geidl M, Koeppel G, Favre-Perrod P, et al. Energy hubs for the future[J]. IEEE power and energy magazine, 2006, 5(1): 24-30.

[5] X. Zhang, M. Shahidehpour, A. Alabdulwahab and A. Abusorrah, "Optimal Expansion Planning of Energy Hub With Multiple Energy Infrastructures," in IEEE Transactions on Smart Grid, vol. 6, no. 5, pp. 2302-2311, Sept. 2015, doi: 10.1109/TSG.2015.2390640.

[6] W. Huang, N. Zhang, J. Yang, Y. Wang and C. Kang, "Optimal Configuration Planning of Multi-Energy Systems Considering Distributed Renewable Energy," in IEEE Transactions on Smart Grid, vol. 10, no. 2, pp. 1452-1464, March 2019, doi: 10.1109/TSG.2017.2767860.

[7] C. Unsihuay-Vila, J. W. Marangon-Lima, A. C. Z. de Souza, I. J. Perez-Arriaga and P. P. Balestrassi, "A Model to Long-Term, Multiarea, Multistage, and Integrated Expansion Planning of Electricity and Natural Gas Systems," in IEEE Transactions on Power Systems, vol. 25, no. 2, pp. 1154-1168, May 2010, doi: 10.1109/TPWRS.2009.2036797.

[8] B. Zhao, A. J. Conejo and R. Sioshansi, "Coordinated Expansion Planning of Natural Gas and Electric Power Systems," in IEEE Transactions on Power Systems, vol. 33, no. 3, pp. 3064-3075, May 2018, doi: 10.1109/TPWRS.2017.2759198.

[9] Zeng Q, Zhang B, Fang J, et al. A bi-level programming for multistage co-expansion planning of the integrated gas and electricity system[J]. Applied energy, 2017, 200: 192-203.

[10] R. Lu, T. Ding, B. Qin, J. Ma, X. Fang and Z. Dong, "Multi-Stage Stochastic Programming to Joint Economic Dispatch for Energy and Reserve With Uncertain Renewable Energy," in IEEE Transactions on Sustainable Energy, vol. 11, no. 3, pp. 1140-1151, July 2020, doi: 10.1109/TSTE.2019.2918269.

[11] C. He, L. Wu, T. Liu and Z. Bie, "Robust Co-Optimization Planning of Interdependent Electricity and Natural Gas Systems With a Joint N-1 and Probabilistic Reliability Criterion," in IEEE Transactions on Power Systems, vol. 33, no. 2, pp. 2140-2154, March 2018, doi: 10.1109/TPWRS.2017.2727859.

[12] Boyd S, Parikh N, Chu E. Distributed optimization and statistical learning via the alternating direction method of multipliers[M]. Now Publishers Inc, 2011.

[13] Lin T, Ma S, Zhang S. Global convergence of unmodified 3-block ADMM for a class of convex minimization problems[J]. Journal of Scientific Computing, 2018, 76(1): 69-88.

[14] C. Shao, X. Wang, M. Shahidehpour, X. Wang and B. Wang, "An MILP-Based Optimal Power Flow in Multicarrier Energy Systems," in IEEE Transactions on Sustainable Energy, vol. 8, no. 1, pp. 239-248, Jan. 2017, doi: 10.1109/TSTE.2016.2595486.

[15] A. Xuan, Dataset for General Synergic and Distributed Planning Models of Natural Gas and Electricity Systems and Integrated Energy Systems (Apr 2021).URL https://figshare.com/s/f54b310eda15a2cb4b4b